SPEEDAM 2006
International Symposium on Power Electronics,
Electrical Drives, Automation and Motion

Design-oriented steady state analysis of LLC resonant converters based on FHA

S. De Simone, C. Adragna, C. Spini and G. Gattavari
STMicroelectronics, via C. Olivetti 2, 20041 Agrate Brianza (MI), (*Italy*)

Abstract **-- The aim of this paper is to present a comprehensive design methodology for an LLC resonant converter, based on a detailed quantitative analysis of the steady-state operation of the circuit. This analysis follows the first harmonic approximation (FHA) approach, which tremendously simplifies the system model, leading to a linear circuit, which can be dealt with through the classical complex ac-circuit analysis.**
Two of the major benefits of the LLC resonant topology are the ability of the Power MOSFETs and secondary rectifiers to be soft-switched and the capability of operating down to zero load. The design-oriented steady-state analysis presented in this paper addresses these two constraints quantitatively, allowing the designer to derive the circuit parameters which not only fulfill input voltage and output power specification data but also soft-switching and no-load operation constraints.

Index Terms **– Ac-circuit analysis, first harmonic approximation, LLC resonant converter, soft-switching, zero-current switching, zero-voltage switching.**

I. Introduction

The LLC resonant converter is recently getting more and more popular in its half-bridge implementation (see figure 1) because of its high efficiency, low level of EMI emissions and its ability to achieve high power density. Such features excellently fit the power supply demand of many modern applications such as LCD and PDP TV or 80+ initiative compliant ATX silver box. It is felt that one of the major difficulties that engineers are facing with this topology is the lack of information concerning the way the converter operates and, thereby, the way to design it in order to get the most of its features.

The purpose of this paper is to provide a detailed quantitative analysis of the steady-state operation of the topology that can be easily translated into a design procedure.

Exact analysis of LLC resonant converters [1] leads to a complex model that cannot be easily used to derive a handy design procedure. R. Steigerwald [2] has described a simplified method, applicable to any resonant topology, based on the assumption that input-to-output power transfer is essentially due to the fundamental Fourier series components of currents and voltages.

This is what is commonly known as "first harmonic approximation" (FHA) technique, which enables the analysis of resonant converters by means of classical complex ac-circuit analysis. This is the approach that has been used in this paper.

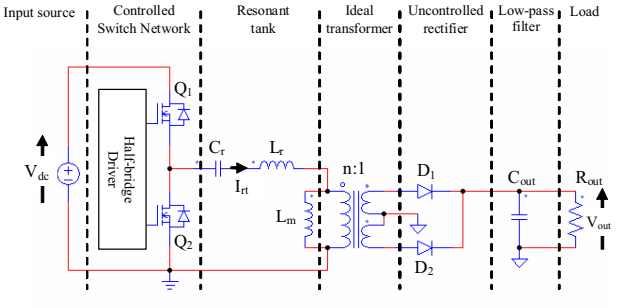

Fig. 1. LLC resonant half-bridge converter

The same methodology has been used by Duerbaum [3] who has highlighted the peculiarities of this topology stemming from its multi-resonant nature. Although providing an analysis useful to set up a design procedure, the quantitative aspect is not fully satisfying since some practical design constraints, especially those related to soft-switching, are not addressed. In [4] a design procedure that optimizes transformer's size is given but, again, many other significant aspects of the design are not considered.

The paper starts with a brief summary of the first harmonic approximation approach, warning of its limitations and highlighting the aspects it cannot predict. Then, the LLC resonant converter is characterized as a two-port element, considering the input impedance, and the forward transfer characteristic. The analysis of the input impedance is useful to determine a necessary condition for Power MOSFETs' ZVS to occur and allows the designer to predict how conversion efficiency behaves when the load changes from the maximum to the minimum value. The forward transfer characteristic (see figure 2) is of great importance to determine the input-to-output voltage conversion ratio and provides considerable insight into converter's operation over the entire range of input voltage and output load. In particular, it provides a simple graphical means to find the condition for the converter to regulate the output voltage down to zero load, which is one of the main benefits of the topology as compared to the traditional series resonant converter.

II. FHA Circuit Model

The FHA approach is based on the assumption that the power transfer from the source to the load through the resonant tank is almost completely associated to the fundamental harmonic of the Fourier expansion of the currents and voltages involved. This is consistent with the selective nature of resonant tank circuits.

1-4244-0194-1/06/$20.00 ©2006 IEEE

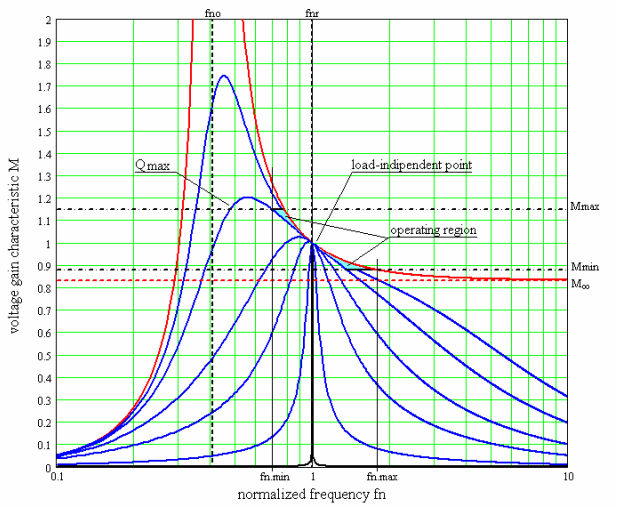

Fig. 2. Conversion ratio of LLC resonant half-bridge

The harmonics of the switching frequency are then neglected and the tank waveforms are assumed to be purely sinusoidal at the fundamental frequency: this approach gives quite accurate results for operating points at and above the resonance frequency of the resonant tank (in the continuous conduction mode), while it is less accurate, but still valid, at frequencies below the resonance (in the discontinuous conduction mode).

It is worth pointing out also that many details of circuit operation on a cycle-to-cycle time base will be lost. In particular, FHA provides only a necessary condition for MOSFETs' zero-voltage switching (ZVS) and does not address secondary rectifiers' natural ability to work always in zero-current switching (ZCS). A sufficient condition for Power MOSFETs' ZVS will be determined in section IV still in the frame of FHA approach.

Let us consider the simple case of ideal components, both active and passive.

The two Power MOSFETs of the half-bridge in figure 1 are driven on and off symmetrically with 50% duty cycle and no overlapping. Therefore the input voltage to the resonant tank $v_{sq}(t)$ is a square waveform of amplitude V_{dc}, with an average value of $V_{dc}/2$. In this case the capacitor C_r acts as both resonant and dc blocking capacitor. As a result, the alternate voltage across C_r is superimposed to a dc level equal to $V_{dc}/2$.

The input voltage waveform $v_{sq}(t)$ of the resonant tank in figure 1 can be expressed in Fourier series:

$$v_{sq}(t) = \frac{V_{dc}}{2} + \frac{2}{\pi} V_{dc} \cdot \sum_{n=1,3,5\ldots} \frac{1}{n} \sin(n\, 2\pi\, f_{sw}\, t) \tag{1}$$

whose fundamental component $v_{i.FHA}(t)$ (in phase with the original square waveform) is:

$$v_{i.FHA}(t) = \frac{2}{\pi} V_{dc} \cdot \sin(2\pi\, f_{sw}\, t) \tag{2}$$

where f_{sw} is the switching frequency. The rms value $V_{i.FHA}$ of the input voltage fundamental component is:

$$V_{i.FHA} = \frac{\sqrt{2}}{\pi} V_{dc} \tag{3}$$

As a consequence of the above mentioned assumptions, the resonant tank current $i_{rt}(t)$ will be also sinusoidal, with a certain rms value I_{rt} and a phase shift Φ with respect to the fundamental component of the input voltage:

$$i_{rt}(t) = \sqrt{2}\, I_{rt} \cdot \sin(2\pi\, f_{sw}\, t - \Phi) = \tag{4}$$

$$= \sqrt{2}\, I_{rt} \cdot \cos\Phi \cdot \sin(2\pi\, f_{sw}\, t) - \sqrt{2}\, I_{rt} \cdot \sin\Phi \cdot \cos(2\pi\, f_{sw}\, t)$$

This current lags or leads the voltage, depending on whether inductive reactance or capacitive reactance dominates in the behavior of the resonant tank in the frequency region of interest. Irrespective of that, $i_{rt}(t)$ can be obtained as the sum of two contributes, the first in phase with the voltage, the second with 90° phase-shift with respect to it.

The dc input current $I_{i.dc}$ from the dc source can also be found as the average value, along a complete switching period, of the sinusoidal tank current flowing during the high side MOSFET conduction time, when the dc input voltage is applied to the resonant tank:

$$I_{i.dc} = \frac{1}{T_{sw}} \cdot \int_0^{T_{sw}/2} i_{rt}(t) \cdot dt = \frac{\sqrt{2}}{\pi} I_{rt} \cdot \cos\Phi \tag{5}$$

where T_{sw} is the time period at switching frequency.

The real power P_{in}, drawn from the dc input source (equal to the output power P_{out} in this ideal case) can now be calculated as both the product of the input dc voltage V_{dc} times the average input current $I_{i.dc}$ and the product of the rms values of the voltage and current's first harmonic, times $\cos\Phi$:

$$P_{in} = V_{dc}\, I_{i.dc} = V_{i.FHA}\, I_{rt} \cdot \cos\Phi \tag{6}$$

the two expressions are obviously equivalent.

The expression of the apparent power P_{app} and the reactive power P_r are respectively:

$$P_{app} = V_{i.FHA}\, I_{rt} \qquad P_r = V_{i.FHA}\, I_{rt} \cdot \sin\Phi \tag{7}$$

Let us consider now the output rectifiers and filter part. In the real circuit, the rectifiers are driven by a quasi-sinusoidal current and the voltage reverses when this current becomes zero; therefore the voltage at the input of the rectifier block is an alternate square wave in phase with the rectifier current of amplitude V_{out}.

The expressions of the square wave output voltage $v_{o.sq}(t)$ is:

$$v_{o.sq}(t) = \frac{4}{\pi} V_o \cdot \sum_{n=1,3,5\ldots} \frac{1}{n} \sin(n\, 2\pi\, f_{sw}\, t - \Psi) \tag{8}$$

which has a fundamental component $v_{o.FHA}(t)$:

$$v_{o.FHA}(t) = \frac{4}{\pi} V_o \cdot \sin(2\pi\, f_{sw}\, t - \Psi) \tag{9}$$

whose rms amplitude is:

$$V_{o.FHA} = \frac{2\sqrt{2}}{\pi} V_{out} \tag{10}$$

where Ψ is the phase shift with respect to the input voltage. The fundamental component of the rectifier current $i_{rect}(t)$ will be:

$$i_{rect}(t) = \sqrt{2}\, I_{rect} \cdot \sin(2\pi\, f_{sw}\, t - \Psi) \tag{11}$$

where I_{rect} is its rms value.

Also in this case we can relate the average output current to the load I_{out} and also derive the ac current $I_{c.ac}$ flowing into the filtering output capacitor:

$$I_{out} = \frac{2}{T_{sw}} \cdot \int_0^{T_{sw}/2} |\, i_{rect}(t)\,| \cdot dt = \frac{2\sqrt{2}}{\pi}\, I_{rect} = \frac{P_{out}}{V_{out}} = \frac{V_{out}}{R_{out}} \tag{12}$$

$$I_{c.ac} = \sqrt{I_{rect}^2 - I_{out}^2} \tag{13}$$

where P_{out} is the output power associated to the output load resistance R_{out}.

Since $v_{o.FHA}(t)$ and $i_{rect}(t)$ are in phase, the rectifier block presents an effective resistive load to the resonant tank circuit, $R_{o.ac}$, equal to the ratio of the instantaneous voltage and current:

$$R_{o.ac} = \frac{v_{o.FHA}(t)}{i_{rect}(t)} = \frac{V_{o.FHA}}{I_{rect}} = \frac{8}{\pi^2}\frac{V_{out}^2}{P_o} = \frac{8}{\pi^2} R_{out} \tag{14}$$

Thus, in the end, we have transformed the non linear circuit of figure 1 into the linear circuit of figure 3, where the ac resonant tank is excited by an effective sinusoidal input source and drives an effective resistive load. This transformation allows the use of complex ac-analysis methods to study the circuit and, furthermore, to pass from ac to dc parameters (voltages and currents), since the relationships between them are well-defined and fixed (see equations (3), (5), (6), (10) and (12) above).

The ac resonant tank in the two-port model of figure 3 can be defined by its forward transfer function H(s) and input impedance $Z_{in}(s)$:

$$H(s) = \frac{V_{o.FHA}(s)}{V_{i.FHA}(s)} = \frac{1}{n} \cdot \frac{n^2 R_{o.ac} \,//\, sL_m}{Z_{in}(s)} \tag{15}$$

$$Z_{in}(s) = \frac{V_{i.FHA}(s)}{I_{rt}(s)} = \frac{1}{sC_r} + sL_r + n^2 R_{o.ac} \,//\, sL_m \tag{16}$$

For the discussion that follows it is convenient to define the effective resistive load reflected to the primary side of the transformer R_{ac}:

$$R_{ac} = n^2 R_{o.ac} \tag{17}$$

and the so-called "normalized voltage conversion ratio" or "voltage gain" $M(f_{sw})$:

$$M(f_{sw}) = n \cdot \left\| H(j\, 2\pi\, f_{sw}) \right\| = n \frac{V_{o.FHA}}{V_{i.FHA}} \tag{18}$$

It can be demonstrated (by applying the relationships (3), (10) and (18) to the circuit in figure 3) that the input-to-output dc-dc voltage conversion ratio is equal to:

$$\frac{V_{out}}{V_{dc}} = \frac{1}{2\,n} \cdot M(f_{.sw}) \tag{19}$$

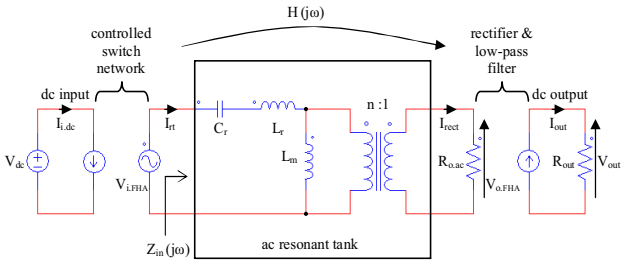

Fig. 3. FHA resonant circuit two port model

In other words, the voltage conversion ratio is equal to one half the module of resonant tank's forward transfer function evaluated at the switching frequency.

III. Voltage Gain And Input Impedance

Starting from (18) we can obtain the expression of the voltage gain:

$$M(f_n, \lambda, Q) = \frac{1}{\sqrt{\left(1 + \lambda - \frac{\lambda}{f_n^2}\right)^2 + Q^2 \cdot \left(f_n - \frac{1}{f_n}\right)^2}} \tag{20}$$

with the following parameter definitions:

resonance frequency: $f_r = \dfrac{1}{2\pi\sqrt{L_r\, C_r}}$

characteristic impedance: $Z_o = \sqrt{\dfrac{L_r}{C_r}} = 2\pi\, f_r L_r = \dfrac{1}{2\pi\, f_r C_r}$

quality factor: $Q = \dfrac{Z_o}{R_{ac}} = \dfrac{Z_o}{n^2\, R_{o.ac}} = \dfrac{Z_o}{n^2}\dfrac{P_{out}}{V_{out}^2}$

inductance ratio: $\lambda = \dfrac{L_r}{L_m}$

normalized frequency: $f_n = \dfrac{f_{sw}}{f_r}$

Under no-load conditions, (i.e. Q = 0) the voltage gain assumes the following form:

$$M_{OL}(f_n, \lambda) = \frac{1}{\left|1 + \lambda - \frac{\lambda}{f_n^2}\right|} \tag{21}$$

Figure 2 shows a family of plots of the voltage gain versus normalized frequency. For different values of Q, with λ = 0.2, it is clearly visible that the LLC resonant converter presents a load-independent operating point at the resonance frequency f_r (f_n = 1), with unity gain, where all the curves are tangent (and the tangent line has a slope –2λ). Fortunately, this load-independent point occurs in the inductive region of the voltage gain characteristic, where the resonant tank lags the input voltage square waveform (which is a necessary condition for ZVS behavior).

The regulation of the converter output voltage is achieved by changing the switching frequency of the

square waveform at the input of the resonant tank: since the working region is in the inductive part of the voltage gain characteristic, the frequency control circuit that keeps the output voltage regulated acts by increasing the frequency in response to a decrease of the output power demand or to an increase of the input dc voltage. Considering this, the output voltage can be regulated against wide loads variations with a relatively narrow switching frequency change, if the converter is operated close to the load-independent point.

Looking at the curves in figure 2, it is obvious that the wider the input dc voltage range is, the wider the operating frequency range will be, in which case it is difficult to optimize the circuit: this is one of the main drawbacks common to all resonant topologies.

This is not the case, however, when there is a PFC pre-regulator in front of the LLC converter, even with a universal input mains voltage ($85V_{ac}$ – $264V_{ac}$). In this case, in fact, the input voltage of the resonant converter is a regulated high voltage bus of ~$400V_{dc}$ nominal, with narrow variations in normal operation, while the minimum and maximum operating voltages will depend, respectively, on the PFC pre-regulator hold-up capability during mains dips and on the threshold level of its over voltage protection circuit (about 10-15% over the nominal value). Therefore, the resonant converter can be optimized to operate at the load-independent point when the input voltage is at nominal value, leaving to the step-up capability of the resonant tank (i.e. operation below resonance) the handling of the minimum input voltage during mains dips.

The red curve in figure 2 represents the no-load voltage gain curve M_{OL}; for normalized frequency going to infinity, it tends to an asymptotic value M_∞:

$$M_\infty = M_{OL}(f_n \to \infty, \lambda) = \frac{1}{1+\lambda} \tag{22}$$

Moreover, a second resonance frequency f_o can be found, which refers to the no-load condition or when the secondary side diodes are not conducting, that is the condition where the total primary inductance $L_r + L_m$ resonates with the capacitor C_r; it is defined as:

$$f_o = \frac{1}{2\pi\sqrt{(L_r + L_m)\,C_r}} = f_r\sqrt{\frac{\lambda}{1+\lambda}} \tag{23}$$

or in normalized form:

$$f_{no} = \frac{f_o}{f_r} = \sqrt{\frac{\lambda}{1+\lambda}} \tag{24}$$

At this frequency the no-load gain curve M_{OL} tends to infinity.

By imposing that the minimum required gain M_{min} (at max. input dc voltage) is greater than the asymptotic value M_∞, it is possible to ensure that the converter can work down to no-load at a finite operating frequency (which will be the maximum operating frequency of the converter):

$$M_{\min} = 2n\cdot\frac{V_{out}}{V_{dc.\max}} > \frac{1}{1+\lambda} \tag{25}$$

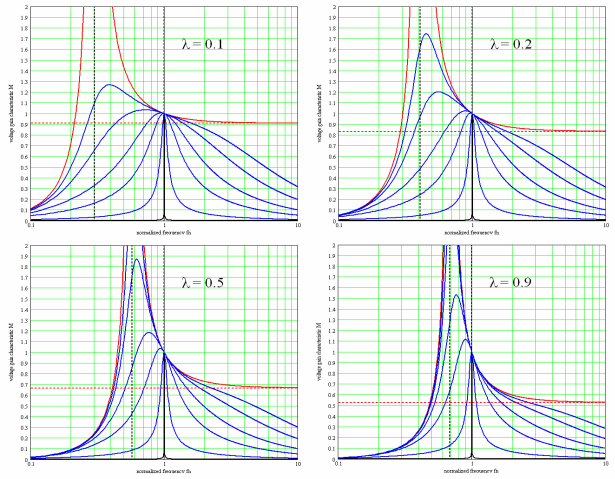

Fig. 4. Shrinking effect of λ value increase

The maximum required gain M_{max} (at min. input dc voltage) at max. output load (max. P_{out}), that is at max. Q, will define the min. operating frequency of the converter:

$$M_{\max} = 2n\cdot\frac{V_{out}}{V_{dc.\min}} \tag{26}$$

Given the input voltage range ($V_{dc.min}$ - $V_{dc.max}$), three types of operation are possible:
- always below resonance frequency (step-up operation)
- always above resonance frequency (step-down operat.)
- across the resonance frequency (shown in figure 2).

Looking at figure 4, we can see that an increase of the inductance ratio value λ has the effect of shrinking the gain curves in the M - f_n plane toward the resonance frequency f_{nr} (which means the no-load resonance frequency f_{no} increases) and contemporarily reduces the asymptotic level M_∞ of the no-load gain characteristic; at the same time the peak gain of each curve increases.

Starting from (16) we can obtain the expression of the normalized input impedance Z_n of the resonant tank:

$$Z_n(f_n,\lambda,Q) = \frac{Z_{in}(\cdot)}{Z_o} = \frac{j\,f_n}{\lambda + j\,f_n\,Q} + \frac{1-f_n^2}{j\,f_n} \tag{27}$$

whose magnitude is plotted in figure 5, at different Q values, with λ = 0.2.

The red and blue curves in the above mentioned figure represent the no-load and short circuit cases respectively, and are characterized by asymptotes at the two normalized resonance frequencies f_{no} and f_{nr} (= 1). All the curves at different values of Q intercept at normalized frequency $f_{n.cross}$:

$$f_{n.cross} = \sqrt{\frac{2\,\lambda}{1+2\,\lambda}} \tag{28}$$

At frequencies higher than the crossing frequency $f_{n.cross}$, the input impedance behaves such that at increasing output current I_{out} (that is at increasing P_{out} and Q) it decreases (coherently to the load resistance); the opposite happens at frequencies lower than $f_{n.cross}$, where the input impedance increases, while the output load resistance decreases.

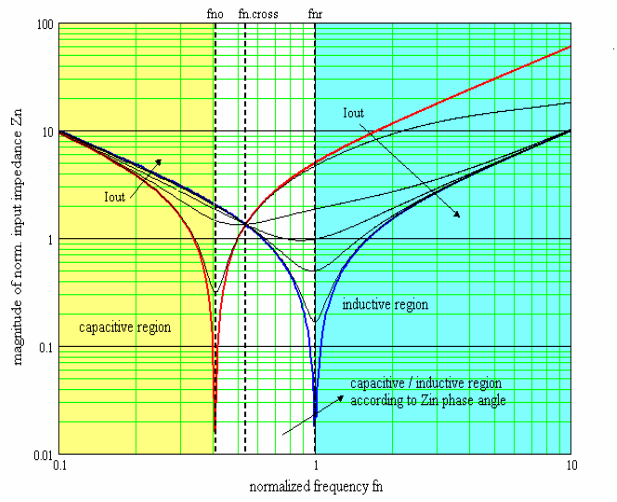

Fig. 5. Normalized input impedance magnitude

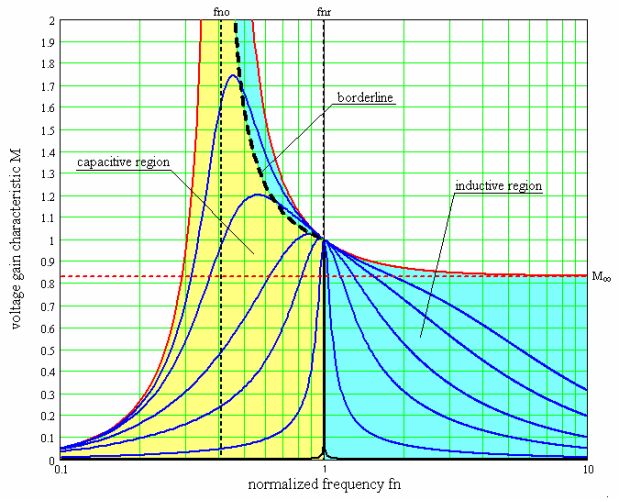

Fig. 6. Capacitive and inductive regions in M – f_n plane

The ac analysis can also help to estimate converter's efficiency η and predict how this changes with the load. Considering the generic model similar to the one in figure 3, where the resonant tank includes also the dissipative elements (i.e. series resistors for magnetic components winding losses and capacitor's ESR, and parallel resistors for magnetic losses of inductors and transformer), we can compute the transfer function $H_{LOSS}(j\omega)$ and the input impedance $Z_{in.LOSS}(j\omega)$. By calculating input and output power in terms of H_{LOSS} and $Z_{in.LOSS}$, we get:

$$\eta = \frac{P_{out}}{P_{in}} = \frac{\left\| H_{LOSS}(j\omega) \right\|^2}{R_{o.ac} \cdot \mathrm{Re}\left[Y_{in.LOSS}(j\omega) \right]} \tag{29}$$

where $Y_{in.LOSS}$ is the admittance (reciprocal of $Z_{in.LOSS}$) and the input and output power are expressed as:

$$P_{in} = V_{i.FHA}\, I_{rt} \cdot \cos\Phi = V_{i.FHA}^2 \cdot \mathrm{Re}\left[\frac{1}{Z_{in.LOSS}(j\omega)} \right] \tag{30}$$

$$P_{out} = V_{o.FHA}\, I_{rect} = \frac{V_{o.FHA}^2}{R_{o.ac}} = \frac{V_{i.FHA}^2}{R_{o.ac}} \cdot \left\| H_{LOSS}(j\omega) \right\|^2 \tag{31}$$

The region on the left-hand side of the diagram in figure 5, i.e. for a normalized frequency lower than f_{no}, is the capacitive region, where the tank current leads the half-bridge square voltage; at normalized frequency higher than the resonance frequency f_{nr} (= 1), on the right-hand side region, the input impedance is inductive, and the resonant tank current lags the input voltage. In the region between the two resonance frequencies the impedance can be either capacitive or inductive, depending on the value of the impedance phase angle.

By imposing that the imaginary part of $Z_n(f_n, \lambda, Q)$ is zero (which means imposing that Z_{in} has zero phase angle, as Z_o is real and does not affect the phase), we can find the boundary condition between capacitive and inductive mode operation of the LLC resonant converter.

The analytical results are the following:

$$f_{nZ}(\lambda, Q) = \sqrt{\frac{Q^2 - \lambda(1+\lambda) + \sqrt{\left[Q^2 - \lambda(1+\lambda)\right]^2 + 4\,Q^2\lambda^2}}{2\,Q^2}} \tag{32}$$

$$Q_Z(f_n, \lambda) = \sqrt{\frac{\lambda}{1+f_n^2} - \left(\frac{\lambda}{f_n}\right)^2} \tag{33}$$

where f_{nZ} represents the normalized frequency where, for a fixed couple (λ - Q), the input resonant tank impedance is real (and only real power is absorbed from the source); while Q_Z is the maximum value of the quality factor, below which, at a fixed normalized frequency and inductance ratio (f_n - λ) the tank impedance is inductive; hence, the maximum voltage gain available in that condition is also found:

$$M_{MAX}(\lambda, Q) = M(f_{nZ}(\lambda, Q), \lambda, Q) \tag{34}$$

By plotting the locus of operating points [$M_{MAX}(\lambda, Q)$, $f_{nZ}(\lambda,Q)$], whose equation on M – f_n plane is the following:

$$M_Z(f_n, \lambda) = \frac{f_n}{\sqrt{f_n^2\,(1+\lambda) - \lambda}} \tag{35}$$

we can draw the borderline between capacitive and inductive mode in the region between the two resonance frequencies, shown in figure 6. It is also evident that the peak value of the gain characteristics for a given quality factor Q value, already lays in the capacitive region.

Moreover, by equating the second term of (35) to the maximum required gain M_{max} (at minimum input voltage), and solving for f_n, we get the minimum operating frequency $f_{n.min}$ which allows the required maximum voltage gain at the boundary between capacitive and inductive mode:

$$f_{n.\min} = \sqrt{\frac{1}{1 + \frac{1}{\lambda}\left(1 - \frac{1}{M_{\max}^2}\right)}} \tag{36}$$

Furthermore, by substituting the minimum frequency (36) into the (33), we get the maximum quality factor Q_{max} which allows the required maximum voltage gain at the boundary between capacitive and inductive mode:

$$Q_{\max} = \frac{\lambda}{M_{\max}} \sqrt{\frac{1}{\lambda} + \frac{M_{\max}^2}{M_{\max}^2 - 1}} \tag{37}$$

Finally, by equating the second term of the no-load transfer function (21) to the minimum required voltage gain M_{min}, it is possible to find the expression of the maximum normalized frequency $f_{n.max}$:

$$f_{n.\max} = \sqrt{\frac{1}{1 + \frac{1}{\lambda}\left(1 - \frac{1}{M_{\min}}\right)}} \tag{38}$$

IV. ZVS Constraints

The assumption that the working region lays inside the inductive region of operation is only a necessary condition for the ZVS of the half bridge MOSFETs, but not sufficient; this is because the parasitic capacitance of the half bridge midpoint, neglected in the FHA analysis, needs some energy to be charged and depleted during transitions. In order to understand the ZVS behavior, refer to the half bridge circuit in figure 7, where the capacitors C_{oss} and C_{stray} are, respectively, the effective drain-source capacitance of the Power MOSFETs and the total stray capacitance present across the resonant tank impedance; so that the total capacitance C_{zvs} at node N is:

$$C_{zvs} = 2\,C_{oss} + C_{stray} \tag{39}$$

which, during transitions, swings by $\Delta V = V_{dc}$. To allow ZVS, the MOSFET driving circuit is such that a dead time T_D is inserted between the end of the ON-time of either MOSFET and the beginning of the ON-time of the other one, so that both are not conducting during T_D.

Due to the phase lag of the input current with respect to the input voltage, at the end of the first half cycle the inductor current I_{rt} is still flowing into the circuit and, therefore it can deplete C_{ZVS} so that its voltage swings from ΔV to zero (it will be vice versa during the second half cycle).

In order to guarantee ZVS, the tank current at the end of the first half cycle (considering the dead time negligible as compared to the switching period, so that the current change is negligible as well) must exceed the minimum value necessary to deplete C_{ZVS} within the dead time interval T_D, which means:

$$I_{zvs} = i_{rt}\left(\frac{T_{sw}}{2}\right) = C_{zvs}\frac{\Delta V}{T_D} = \left(2\,C_{oss} + C_{stray}\right)\frac{V_{dc}}{T_D} \tag{40}$$

This current equals, of course, the peak value of the reactive current flowing through the resonant tank (it is 90° out-of-phase); the one that determines the reactive power level into the circuit:

$$I_{zvs} = \sqrt{2}\,I_{rt} \cdot \sin\Phi \tag{41}$$

Moreover, as the rms component of the tank current associated to the active power is:

$$I_{act} = I_{rt} \cdot \cos\Phi = \frac{P_{in}}{V_{i.FHA}} \tag{42}$$

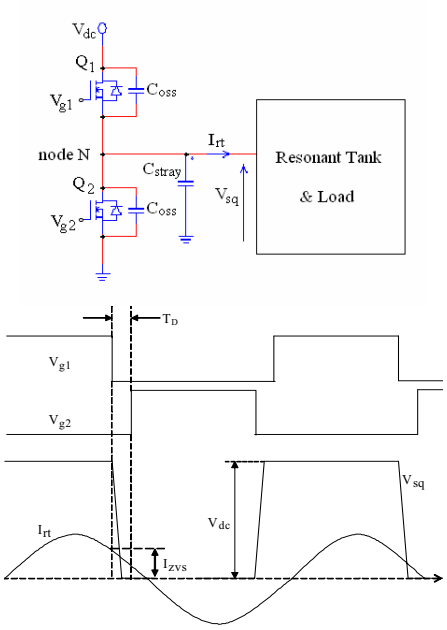

Fig. 7. Circuit behavior at ZVS transition

hence we can derive also the rms value of the resonant tank current and the phase lag Φ between input voltage and current (that is the input impedance phase angle at that operating point):

$$I_{rt} = \sqrt{I_{rt}^2 \cdot \cos^2\Phi + I_{rt}^2 \cdot \sin^2\Phi} = \sqrt{\left(\frac{P_{in}}{V_{i.FHA}}\right)^2 + \frac{I_{zvs}^2}{2}} \tag{43}$$

$$\Phi = a\cos\left(\frac{P_{in}}{V_{i.FHA} \cdot I_{rt}}\right) \tag{44}$$

Thus we can write the following analytic expression:

$$tg(\Phi) = \frac{\mathrm{Im}[Z_n(f_n,\lambda,Q)]}{\mathrm{Re}[Z_n(f_n,\lambda,Q)]} \geq \frac{C_{zvs}}{\pi\,T_D}\frac{V_{dc}^2}{P_{in}} \tag{45}$$

which is the sufficient condition for ZVS of the half-bridge Power MOSFETs, to be applied to the whole operating range. The solution of (45) for the quality factor Q_{zvs} that ensures ZVS behavior at full load and minimum input voltage is not handy. Therefore, we can calculate the Q_{max} value (at max. output power and min. input voltage), where the input impedance has zero phase, and take some margin (5% - 10%) by choosing:

$$Q_{zvs.1} = 90\% \div 95\% \quad \cdot Q_{\max} \tag{46}$$

and check that the condition (45) is satisfied at the end of the process, once the resonant tank has been completely defined. The process will be iterated if necessary.

Of course the sufficient condition for ZVS needs to be satisfied also at no-load and maximum input voltage; in this operating condition it is still possible to find an additional constraint on the maximum quality factor at full load to guarantee ZVS. In fact the input impedance at no-load $Z_{in.OL}$ has the following expression:

$$Z_{in.OL}(f_n) = j \cdot Z_o\left[f_n\left(1 + \frac{1}{\lambda}\right) - \frac{1}{f_n}\right] \tag{47}$$

Taking into account that:

$$Z_o = Q\, R_{ac} \tag{48}$$

and writing the sufficient condition for ZVS in this operating condition, that is:

$$\frac{V_{i.FHA.\max}}{\left\|Z_{in.OL}(f_{n.\max})\right\|} \geq \frac{I_{zvs.@Vdc.maz}}{\sqrt{2}} \tag{49}$$

we get the constraint on the quality factor for the ZVS at no-load and maximum input voltage:

$$Q_{zvs.2} \leq \frac{2}{\pi} \frac{\lambda\, f_{n.\max}}{(\lambda+1) f_{n.\max}^2 - \lambda} \frac{T_D}{R_{ac}\, C_{zvs}} \tag{50}$$

Therefore, in order to guarantee ZVS over the whole operating range of the resonant converter, we have to choose a maximum quality factor value lower than the smaller of $Q_{zvs.1}$ and $Q_{zvs.2}$.

V. Magnetic Integration

The LLC resonant half-bridge lends itself to magnetic integration, i.e. to combine the inductors as well as the transformer into a single magnetic device. This can be easily recognized looking at transformer's physical model (fig. 8), where the topological analogy with the inductive part of the LLC tank circuit is apparent. However, the real transformer has leakage inductance on the secondary side as well, which is completely absent in the model considered so far. To include the effect of secondary leakage in the FHA analysis, we need a particular transformer model and a simplifying assumption.

It is well-known that there are an infinite number of electrically equivalent models of a given transformer, depending on the choice of the turn ratio of the ideal transformer included in the model. With an appropriate choice of this "equivalent" turn ratio n (obviously different from the "physical" turn ratio $n_t = N1/N2$) all the elements related to leakage flux can be located on the primary side.

This is the APR (All-Primary-Referred) model shown in fig. 9, which fits the circuit considered in the FHA analysis. It is possible to show that the APR model is obtained with the following choice of n:

$$n = k \sqrt{\frac{L_1}{L_2}} \tag{51}$$

with k transformer's coupling coefficient, L_1 inductance of the primary winding and L_2 inductance of each secondary winding. Note that L_r still has physical meaning: it is the primary inductance measured with the secondary windings shorted. Note also that the primary inductance L_1 must be unchanged; it is only differently split, hence, L_m will be the difference between L_1 and L_r. In the end, the analysis done so far is directly applicable to real-world transformers provided they are represented by their equivalent APR model. Vice versa, a design flow based on the FHA analysis will provide the parameters of the APR model; hence, an additional step is needed to determine those of the physical model. In particular this applies to the turn number n_t, since L_r and L_m still have a connection with the physical world ($L_r+L_m = L_{L1}+L_\mu=L_1$).

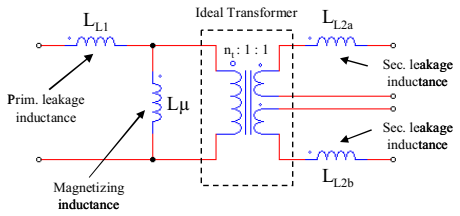

Fig. 8. Transformer's physical model

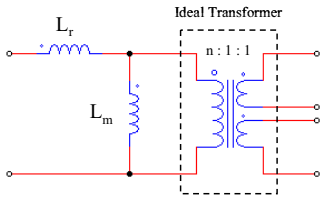

Fig. 9. Transformer's APR (All-Primary-Referred) model

The problem is mathematically undetermined: there are 5 unknowns (L_{L1}, $L\mu$, n_t, and L_{L2a}, L_{L2b}) in the physical model and only three parameters in the APR model. The simplifying assumption that overcomes this issue is that of magnetic circuit symmetry: flux linkage is assumed to be exactly the same for both primary and secondary windings. This provides the two missing conditions:

$$L_{L2a} = L_{L2b} = \frac{L_{L1}}{n_t^2} \tag{52}$$

With this assumption it is now possible to find the relationship between n and n_t:

$$n_t = n \sqrt{\frac{L_m}{L_m + L_r}} = n \sqrt{1+\lambda} \tag{53}$$

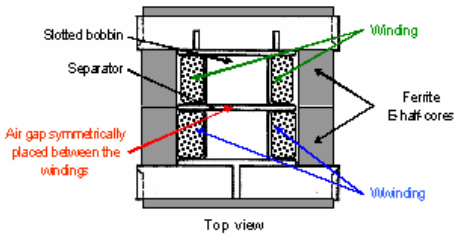

Fig. 10. Transformer construction: E-cores and slotted bobbin

It is not difficult to find real-world structures where the condition of magnetic symmetry is quite close to reality: consider for example the ferrite E-core plus slotted bobbin assembly, using side-by-side winding arrangement, shown in fig. 10.

VI. Design Procedure

Based on the analysis presented so far, a step-by-step design procedure of an LLC resonant converter is now proposed, which fulfills the following design specification and requires the additional information listed below:

- Design Specification:
- Input voltage range: $V_{dc.min} - V_{dc.max}$
- Nominal input voltage: $V_{dc.nom}$
- Regulated output voltage: V_{out}
- Maximum output power: P_{out}
- Resonant frequency: f_r
- Maximum operating frequency: f_{max}

- Additional Info:
- Parasitic capacitance at node N: C_{zvs}
- Dead time of driving circuit: T_D

- General criteria for the design will be the following:
- The converter will be designed to work at resonance at nominal input voltage.
- The converter must be able to regulate down to zero load at maximum input voltage.
- The converter will always work in ZVS in the whole operating range.

Step 1 – to fulfill the first criterion, impose that the required gain at nominal input voltage equals unity and calculate the transformer turn ratio:

$$M_{nom} = 2\,n\,\frac{V_{out}}{V_{dc.nom}} = 1 \quad \Rightarrow \quad n = \frac{1}{2}\,\frac{V_{dc.nom}}{V_{out}}$$

Step 2 – calculate the max. and min. required gain at the extreme values of the input voltage range:

$$M_{\max} = 2\,n\,\frac{V_{out}}{V_{dc.\min}} \qquad M_{\min} = 2\,n\,\frac{V_{out}}{V_{dc.\max}}$$

Step 3 – calculate the maximum normalized operating frequency (according to the definition):

$$f_{n.\max} = \frac{f_{\max}}{f_r}$$

Step 4 – calculate the effective load resistance reflected to transformer primary side, from (14) and (17):

$$R_{ac} = \frac{8}{\pi^2}\,n^2\,\frac{V_{out}^2}{P_{out}}$$

Step 5 – impose that the converter operates at maximum frequency at zero load and maximum input voltage, calculating the inductance ratio from (38):

$$\lambda = \frac{1 - M_{\min}}{M_{\min}}\,\frac{f_{n.\max}^2}{f_{n.\max}^2 - 1}$$

Step 6 – calculate the max Q value to work in the ZVS operating region at minimum input voltage and full load condition, from (37) and (46):

$$Q_{zvs.1} = 95\% \cdot Q_{\max} = 95\% \cdot \frac{\lambda}{M_{\max}}\sqrt{\frac{1}{\lambda} + \frac{M_{\max}^2}{M_{\max}^2 - 1}}$$

Step 7 – calculate the max Q value to work in the ZVS operating region at no-load condition and maximum input voltage, applying (50):

$$Q_{zvs.2} = \frac{2}{\pi}\,\frac{\lambda\, f_{n.\max}}{(\lambda+1)\, f_{n.\max}^2 - \lambda}\,\frac{T_D}{R_{ac}\, C_{zvs}}$$

Step 8 – choose the max quality factor for ZVS in the whole operating range, such that:

$$Q_{zvs} \le \min\{Q_{zvs.1}, Q_{zvs.2}\}$$

Step 9 – calculate the minimum operating frequency at full load and minimum input voltage, according to the following approximate formula:

$$f_{\min} = f_r\,\sqrt{\frac{1}{1 + \frac{1}{\lambda}\left(1 - \frac{1}{M_{\max}^{1+\left(\frac{Q_{zvs}}{Q_{\max}}\right)^4}}\right)}}$$

Step 10 – calculate the characteristic impedance of the resonant tank and all component values (from definition):

$$Z_o = Q\,R_{ac} \qquad C_r = \frac{1}{2\pi\, f_r\, Z_o}$$

$$L_r = \frac{Z_o}{2\pi\, f_r} \qquad L_m = \frac{L_r}{\lambda}$$

VII. Conclusions

The LLC resonant converter, whose peculiarities and advantages have been introduced in the first section, has been modeled as a linear circuit through the FHA technique presented in the second section, where the input controlled switch network, the output rectifiers and filter have been modeled neglecting all the harmonics above the fundamental component of voltages and currents involved. The resulting two-port model is fully characterized by the input impedance $Z_{in}(j\omega)$ and the voltage gain function $M(j\omega)$ of the resonant tank. These two functions have been quantitatively analyzed in the third section, where the conditions to operate on the boundary between capacitive and inductive regions and to regulate down to zero load have been mathematically derived. In the fourth section, the ZVS constraints have been addressed, and a sufficient condition has been found (within the limitations of the FHA approach) to guarantee ZVS even at the extremes of output load and input voltage. In the fifth section the integration of all magnetic parts of the LLC tank into a single transformer has been addressed.

Finally, in the sixth section a simple step-by-step design procedure has been outlined, which enables to fulfill a set of specification data concerning output power and input voltage, as well as ZVS and zero load operation requirements.

References

[1] J.F. Lazar; R. Martinelli: *Steady-state Analysis of the LLC Resonant Converter*, Applied Power Electronics Conference and Exposition, 2001. APEC 2001. Pages: 728 - 735

[2] R.L. Steigerwald: *A Comparison of Half Bridge Resonant Converter Topologies*, IEEE Trans. on Power Electronics, 1988. Pages: 174 - 182.

[3] T. Duerbaum: *First harmonic approximation including design constraints*, Telecommunications Energy Conference, 1998. INTELEC. Pages: 321 – 328

[4] M.B. Borage; S.R. Tiwari; S. Kotaiah: *Design Optimization for an LCL-Type Series Resonant Converter*, http://www.powerpulse.net/features/techpaper.php?paperID=76